Characteristic tetrahedron of wrench singularities for parallel manipulators with three legs

I Ebert-Uphoff[1]*, J-K Lee[2] and H Lipkin[1]
[1]George W Woodruff School of Mechanical Engineering, Georgia Institute of Technology, Atlanta, Georgia, USA
[2]School of Mechanical Engineering, Kunsan National University, Kunsan Chonbuk, Korea

Abstract: A new analysis of wrench singularities is presented for spatial parallel platform manipulators consisting of three legs, with up to two actuators each, and connected to the mobile platform by spherical joints. The analysis also applies to some related manipulators with six legs, such as the 6–3 Gough–Stewart platform. The characteristic tetrahedron is introduced to identify wrench singularities, i.e. configurations where the platform can move infinitesimally with all actuators locked. An important theorem is presented that provides a geometric interpretation of wrench singularities: a manipulator is at a wrench singularity if and only if the characteristic tetrahedron is singular. All cases in which the tetrahedron becomes singular are enumerated, which leads to a classification of wrench singularities. This method is easy to visualize and presents an alternative to standard approaches using line geometry.

Keywords: parallel manipulator, singularity analysis, characteristic tetrahedron, screw theory

NOTATION

$\boldsymbol{a}, \boldsymbol{b}, \boldsymbol{c}, \boldsymbol{d}$ (4×1)	four faces of a tetrahedron expressed in homogeneous coordinates (note: when applied to the characteristic tetrahedron, $\boldsymbol{d}$ always represents the base plane)
$\lvert\boldsymbol{ab}\rvert$	*non-square* determinant of two faces, $\boldsymbol{a}$ and $\boldsymbol{b}$ (see reference [**1**])
$\mathbf{A}_i$ (6×2)	active joint screws for leg i $(i=1,2,3)$
$\mathscr{A}, \mathscr{B}$ (6×6)	two Jacobian matrices as defined by Gosselin and Angeles [**2**]
$\mathbf{e}$ (6×6)	edge matrix of a tetrahedron with faces $\boldsymbol{a}$, $\boldsymbol{b}$, $\boldsymbol{c}$, $\boldsymbol{d}$
$\mathbf{f}$ (6×6)	canonical wrench matrix $=$ $[\boldsymbol{f}_{B1}\ \boldsymbol{f}_{B2}\ \boldsymbol{f}_{B3}\ \boldsymbol{f}_{A1}\ \boldsymbol{f}_{A2}\ \boldsymbol{f}_{A3}]$
$\boldsymbol{f}_{Ai}, \boldsymbol{f}_{Bi}$ (6×1)	pure force wrenches as shown in Fig. 5
$\mathbf{P}_i$ (6×4)	passive joint screws for leg i $(i=1,2,3)$
$\mathbf{T}$ (6×1)	platform twist motion in Plücker axis coordinates
U	arbitrary subspace of vector space V
V	arbitrary vector space
$\boldsymbol{w}_i$ (6×2)	pair of wrenches in Plücker ray coordinates which are *reciprocal* to $\mathbf{P}_i$ for leg i $(i=1,2,3)$
W	arbitrary subspace of vector space V
$\mathbf{W}$ (6×6)	Wrench matrix, $[\boldsymbol{w}_1\ \boldsymbol{w}_2\ \boldsymbol{w}_3]$
$\boldsymbol{\gamma}$ (6×6)	non-singular permutation matrix relating wrench matrix $\mathbf{W}$ to canonical wrench matrix $\mathbf{f}$
$\dot{\boldsymbol{\theta}}_i$ (2×1)	active joint speed for leg i $(i=1,2,3)$
$\dot{\boldsymbol{\varphi}}_i$ (4×1)	passive joint speed for leg i $(i=1,2,3)$

The MS was received on 5 January 2001 and was accepted after revision for publication on 26 April 2001.
* *Corresponding author: George W. Woodruff School of Mechanical Engineering, Georgia Institute of Technology, Atlanta, GA 30332-0405, USA.*

1 INTRODUCTION

The analysis of mechanism singularities is important since they set the limits of kinematic motion and static load equilibration. The singularities of serial mechanisms, such as most industrial robotic manipulators, have been well studied. These limit the motion of the terminal link and are referred to here as *twist singularities*. The singularities of parallel platform devices are less well known and are inherently more complex. They may limit motion of the moving platform (twist singularities) and may limit the ability to equilibrate static loads, which are referred to here as *wrench singularities*. Using

a geometric approach, wrench singularities are investigated for a common class of parallel platform devices with three legs or branches.

In a parallel mechanism, the mobile platform is often connected to the actuating legs through spherical joints or their kinematic equivalents. This means that the loads transmitted to the platform by the legs are pure forces. When the space spanned by these forces reduces in rank, the mechanism is in a wrench singularity. Since forces are screw quantities [**3**], it is natural to use the geometry of screw systems to identify and classify the singularities. However, forces are a unique type of screw since they have a zero pitch. In combination they often form so-called special screw systems which have been identified and well described by Hunt [**4**] and Phillips [**5**, **6**]. Since lines are also zero pitch screws, these particular types of special screw system are treatable by classical line geometry.

Using line geometry, wrench singularity analyses for platform devices have been presented by Collins and Long [**7**], Hao and McCarthy [**8**], Merlet [**9**], Notash [**10**] and others. These articles are based on the line geometry classifications given by Dandurand [**11**]. The basic idea is to determine whether the forces acting on the moving platform belong to one of the line system geometries of rank 5 or less. This identification is typically performed synthetically by considering the possible configurations of the device that can produce the possible line systems. However, this entails visualizing the line geometries and using their unique properties, which is often very difficult.

This paper presents a simplified method of wrench singularity analysis for spatial platform manipulators with three legs that are connected to the moving platform by spherical joints. The key to the analysis is the identification of the characteristic tetrahedron. It is shown that there is a one-to-one relationship between the wrench singularities and the characteristic tetrahedron singularities. In the remainder of the paper, the kinematics of platform singularities are first developed and then the geometrical properties of tetrahedra are detailed. Next, the relationship between wrench singularities and tetrahedron singularities is established. This leads to an enumeration of wrench singularities based on easily identified tetrahedron singularities. Finally, an example is presented that illustrates the method.

2 PLATFORM KINEMATICS

This section develops the first-order kinematic model for the analysis of platform manipulator singularities. The platforms are restricted to having the following characteristics:

1. There are three legs.
2. Each leg is connected to a platform by a spherical or a spherical-equivalent joint (three degrees of freedom).
3. In addition to each spherical joint, each leg has one other passive joint plus two actuated joints (motors).

For greater clarity and without any loss of generality, it is assumed that the spherical joints connect the legs to the moving platform rather than to the fixed base. Each leg has a total of two actuated degrees of freedom and four passive degrees of freedom. Each mechanism has six degrees of freedom controlled by the six actuated joints. Figure 1 shows a sample mechanism, where each leg consists of an RRRS chain. This mechanism is used as the primary example throughout the article. Any two of the three revolute joints of each leg can be selected for actuation.

The basic method is to treat each leg of the platform as a serial chain with active and passive joints. Using reciprocal screws, the passive joints are eliminated, leaving the desired relationship between the platform motion and the active joints. *This investigation differs from most in that a reciprocal two-system is used for elimination rather than two distinct reciprocal screws* (see reference [**12**]). Formally, this results in a block diagonal matrix rather than a diagonal matrix multiplying the active joint rates. However, conceptually, this facilitates the geometric development of the characteristic tetrahedron used for the singularity analysis.

2.1 Extension of the considered class of mechanisms

The legs may be serial chains or contain closed-loop chains. This includes any six-legged mechanism for

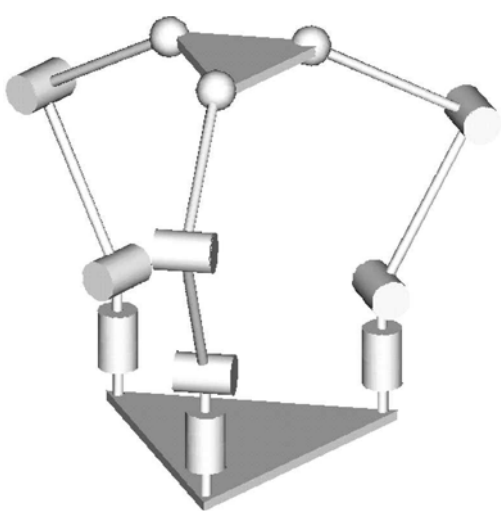

Fig. 1 Prototype manipulator with three legs connected to the moving platform through spherical joints

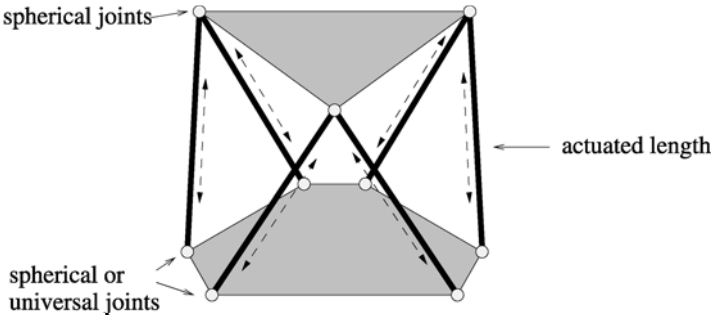

Fig. 2 6–3 Gough–Stewart platform

which pairs of legs kinematically meet in a single spherical joint. An example is the 6–3 Gough–Stewart platform shown in Fig. 2, which is also known as the TSSM mechanism [**13**].

Mechanisms with three legs but fewer than six degrees of freedom can also be included in the analysis. The fundamental criterion is that, when the actuators of a leg are locked, there are exactly two independent reaction forces through the spherical joint. To implement the method for legs with fewer than six degrees of freedom, virtual actuated joints that are locked are added so that the number of actuated joints in each leg is exactly two. By this means, requirement 3 can be relaxed to the following:

3′. In addition to each spherical joint, each leg has one passive joint plus zero, one or two actuated joints.

For example, the spatial mechanism by Lee and Shah [**14**] has three legs, each consisting of an RPS chain. Only the prismatic joints are actuated, resulting in a mechanism with three degrees of freedom. For our analysis, each leg is modelled as an RRPS chain, where the first revolute joint is an actuated joint that is locked.

2.2 Leg model

Figure 1 illustrates a platform manipulator prototype. Each leg is modelled as a serial chain:

$$\mathbf{T} = [\mathbf{A}_i \; \mathbf{P}_i] \begin{bmatrix} \dot{\boldsymbol{\theta}}_i \\ \dot{\boldsymbol{\varphi}}_i \end{bmatrix} = \mathbf{A}_i \dot{\boldsymbol{\theta}}_i + \mathbf{P}_i \dot{\boldsymbol{\varphi}}_i, \qquad i = 1, 2, 3 \tag{1}$$

where i counts the legs, $\mathbf{T}\ (6 \times 1)$ is the platform twist motion in Plücker axis coordinates, $\mathbf{A}_i\ (6 \times 2)$ and $\mathbf{P}_i\ (6 \times 4)$ are the active and passive joint screws and $\dot{\boldsymbol{\theta}}_i\ (2 \times 1)$ and $\dot{\boldsymbol{\varphi}}_i\ (4 \times 1)$ are the active and passive joint speeds. In the case where legs contain closed-loop chains, some of the screws in (1) correspond to virtual joints.

2.3 Platform model

For each leg, let $\boldsymbol{w}_i\ (6 \times 2)$ be a pair of wrenches in Plücker ray coordinates that are *reciprocal* to the passive joint screws, i.e. $\boldsymbol{w}_i^{\mathrm{T}} \mathbf{P}_i = \mathbf{0}$. Eliminating the passive quantities in (1) by multiplying by $\boldsymbol{w}_i^{\mathrm{T}}$ from the left and combining the results gives the desired relationship between the platform and active joint motions:

$$\underbrace{\begin{bmatrix} \boldsymbol{w}_1 & \boldsymbol{w}_2 & \boldsymbol{w}_3 \end{bmatrix}^{\mathrm{T}}}_{(6\times 6)} \underbrace{\begin{bmatrix} \mathbf{T} \end{bmatrix}}_{(6\times 1)} = \underbrace{\begin{bmatrix} \boldsymbol{w}_1^{\mathrm{T}}\mathbf{A}_1 & & \\ & \boldsymbol{w}_2^{\mathrm{T}}\mathbf{A}_2 & \\ & & \boldsymbol{w}_3^{\mathrm{T}}\mathbf{A}_3 \end{bmatrix}}_{(6\times 6)} \underbrace{\begin{bmatrix} \dot{\boldsymbol{\theta}}_1 \\ \dot{\boldsymbol{\theta}}_2 \\ \dot{\boldsymbol{\theta}}_3 \end{bmatrix}}_{(6\times 1)} \tag{2}$$

where

$$\mathbf{W} \equiv [\boldsymbol{w}_1 \; \boldsymbol{w}_2 \; \boldsymbol{w}_3] \tag{3}$$

is the (6×6) *wrench matrix* and the matrix on the right has (2×2) blocks on the diagonal. Equation (2) describes the relationship between the actuator velocities and the velocity of the mobile platform. Equation (2) is equivalent to the common notation $\mathscr{A}\,\dot{\boldsymbol{X}} + \mathscr{B}\,\dot{\boldsymbol{\theta}} = \mathbf{0}$ introduced by Gosselin and Angeles [**2**], where in equation (2) the two Jacobian matrices $\mathscr{A}$ and $\mathscr{B}$ are written in convenient screw form.

2.4 Wrench and twist singularities

There are two types of singularities that can be identified from (2):

1. A *twist singularity* occurs if the matrix on the right-hand side of (2) is singular, i.e. at least one term $(\boldsymbol{w}_i^{\mathrm{T}}\mathbf{A}_i)$ is singular for $i = 1, 2, 3$. In this case the actuators of leg i can move instantaneously with

$\dot{\boldsymbol{\theta}}_i \neq \mathbf{0}$, while the mobile platform is stationary, $\mathbf{T} = \mathbf{0}$. As a result, the ith leg loses at least one degree of freedom in a twist singularity and in turn restricts the motion of the mobile platform by at least one degree of freedom. Since a twist singularity arises from the limited motion of a leg, it is often referred to as a *leg singularity*. Twist singularities are identical to the singularities encountered for serial manipulators. Since twist singularities for serial manipulators have been well studied and are relatively easy to locate, they are not further considered in the analysis.

2. A *wrench singularity* occurs if and only if the wrench matrix $\mathbf{W}$ is singular:

$$\det |\mathbf{W}| = 0 \tag{4}$$

In this case the mobile platform is able to move instantaneously, $\mathbf{T} \neq \mathbf{0}$, even if all actuators are immobilized, $\dot{\boldsymbol{\theta}}_i = \mathbf{0}$ for all i. This implies that the platform cannot equilibrate one or more applied wrenches. Wrench singularities are also often referred to as *platform singularities*. They only exist for parallel mechanisms and not for serial mechanisms. When a manipulator gets close to a wrench singularity, the actuator torques required to maintain the configuration for an arbitrary wrench applied at the end-effector may grow indefinitely. In practice this means that the actual motion of the mobile platform cannot be controlled and the mechanism could collapse near large motion singularities. Wrench singularities should be avoided under any circumstances, either at the motion planning level or at the design level.

3 CHARACTERISTIC TETRAHEDRON

This section introduces the characteristic tetrahedron and relates it to the wrench matrix $\mathbf{W}$. After developing the geometric properties of tetrahedra, it is shown how characteristic tetrahedra singularities are equivalent to wrench singularities. However, an indirect approach is taken by first relating non-singular characteristic tetrahedra to non-singular wrench matrices.

3.1 Force pencils

Through each spherical joint, only forces (no moments) can be transmitted to the mobile platform. Furthermore, at any instant, each leg can only generate forces that are spanned by two linearly independent forces $\boldsymbol{w}_i$ through the spherical joint of leg i (see Fig. 3). These forces*, which lie in a plane through the spherical joint, are known as a force *pencil* and are special two-systems of screws [**4–6**]. They are reciprocal to the four passive joints of the leg.

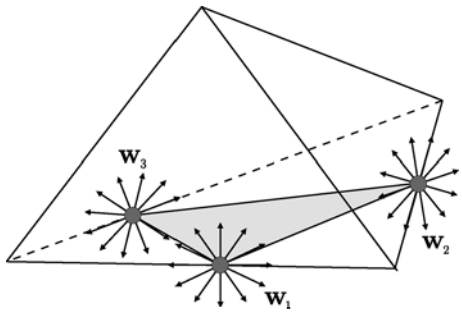

Fig. 3 Non-singular characteristic tetrahedron with a finite apex. Each $\boldsymbol{w}_i$ spans a planar pencil of forces through the ith spherical joint. The plane of each pencil forms one of the three sides, and the plane of the platform forms the base

Combining the planes of the three pencils with the mobile platform plane through the spherical joints defines the characteristic tetrahedron (see Fig. 3).

Definition 1

The *characteristic tetrahedron* is defined by four *faces*: the face specified by the mobile platform is called the *base* and the remaining three faces specified by the planes of the force pencils are called the *sides*. The intersection of the three sides is called the *apex*.

For the purposes of analysis, it is useful to define a tetrahedron and its features in terms of projective geometry.

Definition 2

A *tetrahedron* is the figure of four planes. Each plane is called a *face*. Each pair of faces intersect in an *edge*. Each triplet of faces intersect in a *vertex*.

This definition covers finite elements as well as infinitely distant elements such as the edge of two parallel faces. It is also possible to delineate between non-singular and singular tetrahedra projectively with the following definition.

Definition 3

A tetrahedron is non-singular if and only if its four faces do not have a common point.

Figure 3 is an example of a non-singular tetrahedron with a finite apex. Figure 4a is an example of a non-

* In practice, the two linearly independent forces represented by $\boldsymbol{w}_i$ can easily be determined geometrically for many leg types, as shown in several examples in Section 5.1 (see Figs 7 and 8). The reader may choose to review these examples first before proceeding with Section 3.1.

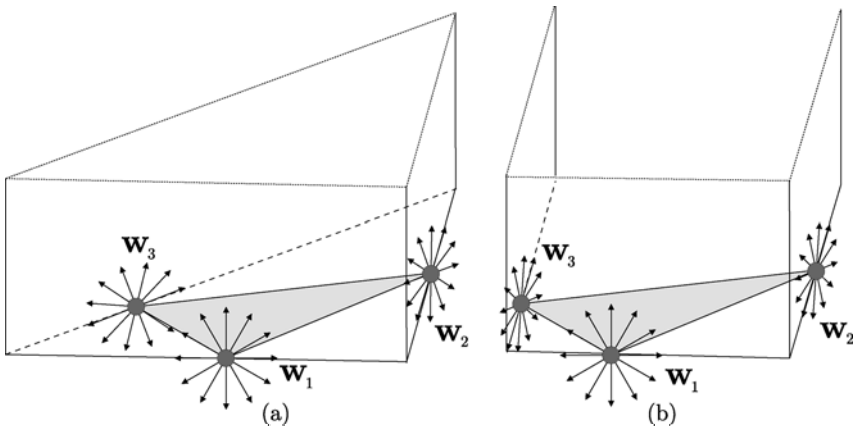

Fig. 4 Non-singular characteristic tetrahedra with infinite elements: (a) three parallel edges with the apex at infinity; (b) one edge at infinity and the apex at infinity

singular tetrahedron with an infinitely distant apex that is the intersection of the three parallel vertical edges. Figure 4b is an example of a non-singular tetrahedron with an infinitely distant apex and an edge at infinity. Singular tetrahedra have a greater variety of forms and are detailed subsequently. The following few sections develop the projective geometry tools required to relate the characteristic tetrahedron to the wrench matrix.

3.2 Plane coordinates

The equation of a plane in homogeneous coordinates is given by

$$a_1x_1 + a_2x_2 + a_3x_3 + a_4x_4 = 0 \tag{5}$$

or $\boldsymbol{a}^{\mathrm{T}}\boldsymbol{x} = 0$, where $\boldsymbol{a}$ represents the homogeneous coordinates of the plane and $\boldsymbol{x}$ represents the homogeneous coordinates of a point [the corresponding inhomogeneous coordinates of a point are $(x_1\ x_2\ x_3)/x_4$]. The equation establishes points $\boldsymbol{x}$ that are incident to plane $\boldsymbol{a}$. Let $\boldsymbol{a}$, $\boldsymbol{b}$, $\boldsymbol{c}$ and $\boldsymbol{d}$ represent the four faces of a tetrahedron and consider

$$[\boldsymbol{a}\ \boldsymbol{b}\ \boldsymbol{c}\ \boldsymbol{d}]^{\mathrm{T}}\boldsymbol{x} = \boldsymbol{0} \tag{6}$$

If the only solution is $\boldsymbol{x} = \boldsymbol{0}$, then there is no point common to the four faces and the tetrahedron is non-singular. (Note that for homogeneous coordinates $\boldsymbol{0}$ does not represent the coordinates of any point.) If there exists a (finite or infinite) point $\boldsymbol{x} \neq \boldsymbol{0}$, then the four faces contain a common point and the tetrahedron is singular. This establishes the following theorem.

Theorem 1

A tetrahedron is non-singular if and only if the determinant of its four faces is non-zero, $|\boldsymbol{a}\ \boldsymbol{b}\ \boldsymbol{c}\ \boldsymbol{d}| \neq 0$.

3.3 Line coordinates

The Plücker (ray) line coordinates of an edge formed by the intersection of the two faces $\boldsymbol{a}$ and $\boldsymbol{b}$ is given by the *non-square* determinant $|\boldsymbol{ab}|$ (see reference [**1**]). This is a 6×1 matrix of subdeterminants specified as

$$|\boldsymbol{ab}| \equiv [\,|a_2b_3|\ |a_3b_1|\ |a_1b_2|\ |a_4b_1|\ |a_4b_2|\ |a_4b_3|\,]^{\mathrm{T}} \tag{7}$$

where $|a_ib_j| \equiv a_ib_j - a_jb_i$. If $|\boldsymbol{ab}|$ vanishes it means that the faces are coincident.

The six edges of a tetrahedron are expressed as the 6×6 edge matrix (see Fig. 5):

$$\mathbf{e} = [\,|\boldsymbol{ad}|\ |\boldsymbol{bd}|\ |\boldsymbol{cd}|\ |\boldsymbol{ab}|\ |\boldsymbol{bc}|\ |\boldsymbol{ca}|\,] \tag{8}$$

The determinants of the faces and the edges are related by the following theorem and can be verified by a

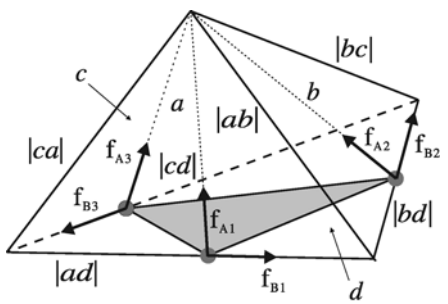

Fig. 5 Non-singular characteristic tetrahedron showing forces along the base and to the vertex

symbolic manipulation program or analytically as shown in reference [**15**].

Theorem 2

The determinant of the edges and the determinant of the faces are related by

$$(\det\ \mathbf{e})^2 = (\det[\boldsymbol{a}\ \boldsymbol{b}\ \boldsymbol{c}\ \boldsymbol{d}])^6$$

This leads to the following corollary.

Corollary

A tetrahedron is non-singular if and only if the determinant of its six edges is non-zero, $\det \mathbf{e} \neq 0$.

In the following section, the edge matrix $\mathbf{e}$ is related to the wrench matrix $\mathbf{W}$.

3.4 Wrench and edge matrices

In the selection of the wrench matrix, each $\boldsymbol{w}_i$ consists of any two forces through the ith spherical joint that are reciprocal to the four passive joints of the ith leg. For non-singular tetrahedra it is always possible to select two unique forces that simplify the analysis

$$\boldsymbol{w}_i = [\boldsymbol{f}_{\mathrm{A}i}\ \boldsymbol{f}_{\mathrm{B}i}] \tag{9}$$

where $\boldsymbol{f}_{\mathrm{A}i}$ points to the tetrahedron apex and $\boldsymbol{f}_{\mathrm{B}i}$ points along the tetrahedron base (see Fig. 5). When the apex is infinitely distant, all of the $\boldsymbol{f}_{\mathrm{A}i}$ are parallel. It is useful to define the canonical wrench matrix as

$$\mathbf{f} = [\,\boldsymbol{f}_{\mathrm{B1}}\ \boldsymbol{f}_{\mathrm{B2}}\ \boldsymbol{f}_{\mathrm{B3}}\ \boldsymbol{f}_{\mathrm{A1}}\ \boldsymbol{f}_{\mathrm{A2}}\ \boldsymbol{f}_{\mathrm{A3}}\,]$$

which is clearly a permutation of the wrench matrix

$$\mathbf{f} = \mathbf{W}\boldsymbol{\gamma} \tag{10}$$

where $\boldsymbol{\gamma}$ is a (6×6) non-singular permutation matrix. The relationship between the wrench matrix and edge matrix is established by the following theorem.

Theorem 3

Wrench matrix $\mathbf{W}$ is non-singular if and only if the edge matrix $\mathbf{e}$ is non-singular.

Proof. This is shown by establishing a non-singular linear transformation $\boldsymbol{\delta}'$ between the non-singular wrench matrix $\mathbf{W}$ and the non-singular edge matrix $\mathbf{e}$:

$$\mathbf{W} = \mathbf{e}\boldsymbol{\delta}' \tag{11}$$

However, since $\mathbf{f} = \mathbf{W}\boldsymbol{\gamma}$ it is sufficient to find a non-singular transformation $\boldsymbol{\delta}$ between $\mathbf{f}$ and $\mathbf{e}$

$$\mathbf{f} = \mathbf{e}\boldsymbol{\delta} \tag{12}$$

where $\boldsymbol{\delta} = \boldsymbol{\gamma}^{-1}\boldsymbol{\delta}'$. Referring to Fig. 5, where $\boldsymbol{d}$ is the base plane, $\boldsymbol{\delta}$ is shown to have the block diagonal form

$$\boldsymbol{\delta} = \begin{bmatrix} \boldsymbol{\beta} & \mathbf{0} \\ \mathbf{0} & \boldsymbol{\alpha} \end{bmatrix} \tag{13}$$

The three forces $\boldsymbol{f}_{\mathrm{B1}}$, $\boldsymbol{f}_{\mathrm{B2}}$ and $\boldsymbol{f}_{\mathrm{B3}}$ along the base are scalar multiples of the lines $|\boldsymbol{ad}|$, $|\boldsymbol{bd}|$ and $|\boldsymbol{cd}|$ along those edges, so $\boldsymbol{\beta}$ is diagonal with non-zero elements. The three forces $\boldsymbol{f}_{\mathrm{A1}}$, $\boldsymbol{f}_{\mathrm{A2}}$ and $\boldsymbol{f}_{\mathrm{A3}}$ to the apex and the three edges $|\boldsymbol{ab}|$, $|\boldsymbol{bc}|$ and $|\boldsymbol{ca}|$ to the apex each form a linearly independent basis for the same space, the set of all forces or lines through the apex, which is a special three-system of screws [**4–6**]. Thus, $\boldsymbol{\alpha}$ is the non-singular transformation between them that produces a change of basis. Therefore the existence of $\boldsymbol{\delta}$ is established. Note that this proof holds for both a finite apex and an infinite apex. In the latter case all the forces and lines to the apex are parallel.

Combining the results of the above Corollary and Theorem 3 gives the following theorem.

Theorem 4

A platform manipulator is in a (wrench) non-singular configuration if and only if the characteristic tetrahedron is non-singular.

Finally, taking the logically equivalent contrapositive statement of Theorem 4 gives the following main result.

Theorem 5

A platform manipulator is in a wrench singularity if and only if the characteristic tetrahedron is singular.

This theorem is used in the remainder of the paper to analyse platform singularities.

4 ENUMERATION OF SINGULAR CONFIGURATIONS

According to Theorem 5, there is a one-to-one relationship between wrench singularities and characteristic tetrahedron singularities. It is therefore proposed to classify wrench singularities by the corresponding characteristic tetrahedron singularities. The singularities are enumerated in four steps and are listed in Table 1.

Firstly, the singularities of general tetrahedra are identified when the matrix of plane coordinates $[\boldsymbol{a}\ \boldsymbol{b}\ \boldsymbol{c}\ \boldsymbol{d}]$ becomes rank deficient, i.e. when the rank of the matrix

Table 1 Enumeration of platform singularities

Case	Rank/deficiency	Reduction	Rank deficiency description	Figure	Line system
1	3/1	$[\boldsymbol{a\ b\ c\ d}]_3$	Four faces meet in a point	6a	5a
2	3/1	$[(\boldsymbol{a\ b\ c})_2\ \boldsymbol{d}]_3$	Three sides meet in a line	6b	5b
3	3/1	$[(\boldsymbol{a\ b\ d})_2\ \boldsymbol{c}]_3$	Two sides and base meet in a line	6c	5a
4	3/1	$[(\boldsymbol{a\ b})_1\ \boldsymbol{c\ d}]_3$	Two sides meet in a plane	6d	5b
5	3/1	$[(\boldsymbol{a\ d})_1\ \boldsymbol{b\ c}]_3$	One side and base meet in a plane	6e	5b
a*	2/2	$[\boldsymbol{a\ b\ c\ d}]_2$	(*Four faces meet in a line*)		
b*	2/2	$[(\boldsymbol{a\ b})_1\ \boldsymbol{c\ d}]_2$	(*Four faces meet in a line*) (*Two sides meet in a plane*)		
6	2/2	$[(\boldsymbol{a\ d})_1\ \boldsymbol{b\ c}]_2$	Four faces meet in a line One side and base meet in a plane	6f	5b
7	2/2	$[(\boldsymbol{a\ b})_1\ (\boldsymbol{c\ d})_1]_2$	Two sides meet in a plane One side and base meet in a plane	6g	5b
c*	2/2	$[(\boldsymbol{a\ b\ c})_1\ \boldsymbol{d}]_2$	(*Three sides meet in a plane*)		
8	2/2	$[(\boldsymbol{a\ b\ d})_1\ \boldsymbol{c}]_2$	Two sides and base meet in a plane	6h	4d
9	1	$[\boldsymbol{a\ b\ c\ d}]_1$	Four faces meet in a plane	6i	3d

* Physically unrealizable.

is less than the number of its columns. There are three primary classifications by rank:

1. The rank is 3, i.e. the four planes meet in a single point.
2. The rank is 2, i.e. the four planes meet in a single line.
3. The rank is 1, i.e. the four planes meet in a single plane.

Secondly, within each rank criterion it is possible for further rank reduction among a subset of the elements without affecting the overall rank of the matrix. A notation analogous to that used by Lipkin and Pohl [**16**] for serial manipulators is introduced to facilitate the enumeration and is explained by examples. If the four planes meet in a single point (rank 3) but additionally three of the planes meet in a single line (rank 2 subset), then it is indicated by $[(\boldsymbol{a\ b\ c})_2\ \boldsymbol{d}]_3$, so the overall rank is given by the outside subscript 3 and the rank of the subset of planes $(\boldsymbol{a\ b\ c})$ is indicated by the subscript 2. In contrast, $[\boldsymbol{a\ b\ c\ d}]_3$ indicates that all four planes meet in a single point but there are no rank reductions among the subsets, i.e. no three planes meet in a line, e.g. $(\boldsymbol{a\ b\ c})_2$, and no two planes meet in a plane, e.g. $(\boldsymbol{a\ b})_1$. There are eight distinct cases without duplications of symmetry, namely $[\boldsymbol{a\ b\ c\ d}]_3$, $[(\boldsymbol{a\ b\ c})_2\ \boldsymbol{d}]_3$, $[(\boldsymbol{a\ b})_1\ \boldsymbol{c\ d}]_3$, $[\boldsymbol{a\ b\ c\ d}]_2$, $[(\boldsymbol{a\ b})_1\ \boldsymbol{c\ d}]_2$, $[(\boldsymbol{a\ b})_1\ (\boldsymbol{c\ d})_1]_2$, $[(\boldsymbol{a\ b\ c})_1\ \mathbf{d}]_2$ and $[\boldsymbol{a\ b\ c\ d}]_1$. These cases are listed in Table 1 as cases 1, 2, 4, a*, b*, 7, c* and 9 respectively.

Thirdly, the characteristic tetrahedron is asymmetrical since the base plane is distinguished from the others. Base plane $\boldsymbol{d}$ always contains three spherical joints, whereas planes $\boldsymbol{a}, \boldsymbol{b}, \boldsymbol{c}$ may contain one, two or three spherical joints depending on the configuration of the manipulator. This identifies four additional cases, namely $[(\boldsymbol{a\ b\ d})_2\ \boldsymbol{c}]_3$, $[(\boldsymbol{a\ d})_1\ \boldsymbol{b\ c}]_3$, $[(\boldsymbol{a\ d})_1\ \boldsymbol{b\ c}]_2$ and $[(\boldsymbol{a\ b\ d})_1\ \boldsymbol{c}]_2$. These cases are listed in Table 1 as cases 3, 5, 6 and 8 respectively.

Fourthly, the generated cases are examined to determine if they are consistent with the constraint that the base plane $\boldsymbol{d}$ always contains three spherical joints. This eliminates three possible cases as unrealizable, namely cases a*, b* and c*.

The remaining nine distinct realizable singular configurations are shown in Figs 6a to i and are referred to in the penultimate column of Table 1. For comparison purposes, the last column of the table contains the classification used by Merlet [**9**] based on line geometry.

5 APPLICATION OF THE SINGULARITY ANALYSIS

A practical platform manipulator presented in reference [**17**] is analysed for its wrench singularities using the characteristic tetrahedron and the enumeration scheme. Effectively, each leg of the manipulator contains three revolute joints and one spherical joint, similar to Fig. 1, but uses a parallelogram mechanism, so that all actuators can be placed at the base for practical implementation (Fig. 7). This leg contains the equivalent leg of Fig. 1 as a special case of actuator placement.

The leg configuration is described by the three independent angles θ_1, θ_2 and θ_3. Please note that notation θ_i is distinct from $\boldsymbol{\theta}_i$ used in Section 2. Angle θ_1 is the rotation of the leg about the vertical z axis. Angles θ_2 and θ_3 are rotations with axes parallel to the horizontal plane.

For each leg the spherical joint and one of the revolute joints are passive and the remaining two revolute joints are actuated. Depending on which joints are actuated, a number of different mechanisms arise. Four different actuator placements are considered:

1. Angles θ_1 and θ_2 are actuated.
2. Angles θ_1 and θ_3 are actuated.
3. Angles θ_2 and θ_3 are actuated.

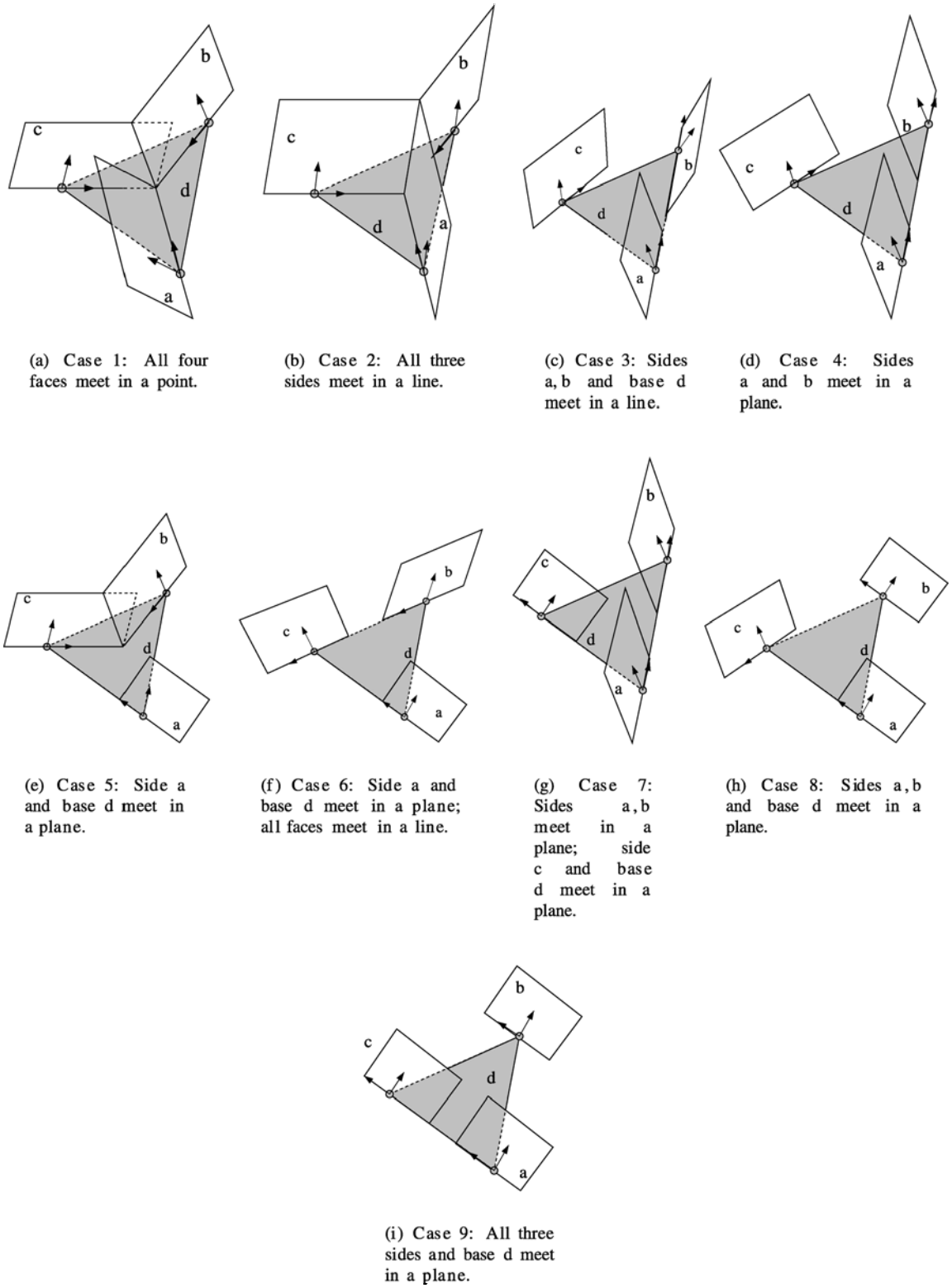

Fig. 6 Singular cases—the four faces have a common (finite or infinite) point

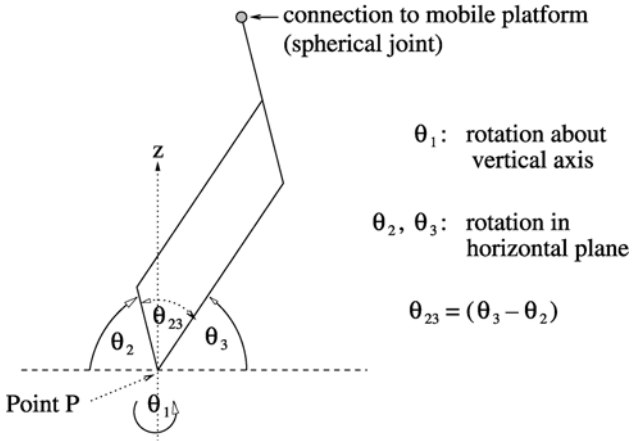

Fig. 7 Model of an individual leg with all actuators at the base

4. Angles θ_1 and θ_{23} are actuated, where θ_{23} is the angle between two sides of the parallelogram, i.e. $\theta_{23} = \theta_3 - \theta_2$.

These different actuation schemes produce distinct singularity properties (see, for example, reference [**18**]).

5.1 Calculation of the characteristic tetrahedron

The force plane at each spherical joint depends on which revolute joint is passive. To determine the force planes (corresponding to $\boldsymbol{w}_i$), the wrenches that are reciprocal to the actuator freedoms are determined by considering a single leg as follows:

1. Immobilize the two actuated joints.
2. Analyse the remaining single degree of freedom and select two reaction forces at the spherical joint. These are reciprocal wrenches, $\boldsymbol{w}_i$, to the unactuated freedom.

Figure 8 shows all four actuator placements when the two actuated angles are immobilized and also shows the remaining degree of freedom. The rigid elements in the figure indicate angles that are fixed. The reaction forces are $\boldsymbol{f}_A$ and $\boldsymbol{f}_B$, and in cases (a), (b) and (d) note that $\boldsymbol{f}_B$ is normal to the parallelogram plane.

Figure 9 shows the whole manipulator with the three resulting force planes for the four different actuator placements. The three force planes shown for each manipulator constitute the three sides, $\boldsymbol{a}$, $\boldsymbol{b}$, $\boldsymbol{c}$, of the characteristic tetrahedron. The fourth face is given by the plane of the mobile platform which constitutes the base, $\boldsymbol{d}$, of the characteristic tetrahedron.

Theorem 5 states that each manipulator is in a singular configuration if and only if the characteristic tetrahedron is singular. For the configurations shown in Fig. 9 it is apparent that the characteristic tetrahedron is only singular in Fig. 9c, where the manipulator is in the singular configuration identified as case 2 in Table 1, since the three sides meet in a line.

The construction of the characteristic tetrahedron is explained for several other mechanisms below:

1. Mechanism by Lee and Shah [**14**]. The actuation scheme shown in Fig. 8d results in a leg equivalent to an RRPS chain, for which the prismatic joint and the vertical revolute joint are actuated. By locking the vertical revolute joint, i.e. by keeping θ_1 constant, the three-degree-of-freedom manipulator by Lee and Shah [**14**] is obtained and can be analysed as shown in Fig. 9d.
2. 6–3 Gough–Stewart platform. For the 6–3 Gough–Stewart platform shown in Fig. 2, each pair of legs that meet at one of the three spherical joints defines a plane through the spherical joint. These three planes are the sides of the characteristic tetrahedron. The fourth plane is given by the mobile platform.
3. 'Mixed manipulator'. The analysis can also be applied to a manipulator with three legs of the type shown in Fig. 7, for which two of the legs are connected to the mobile platform through spherical joints, but the spherical joint of the third leg is located at the connection to the fixed base (i.e. the third leg is turned upside down). In this case the three sides of the characteristic tetrahedron are located at the three spherical joints (regardless of their location). The base plane $\boldsymbol{d}$ is the plane through the three spherical joints.

5.2 Enumeration example

The singularities of a platform manipulator based on the leg mechanism in Fig. 8c are investigated further. Joints θ_2 and θ_3 are actuated while the rotation of each leg about its vertical axis, θ_1, is unactuated. For this actuator placement, the reaction forces $\boldsymbol{f}_A$ and $\boldsymbol{f}_B$ at the spherical joints lie in the plane of the parallelogram which is always orthogonal to the horizontal lower platform (the fixed manipulator base is used here as a horizontal reference plane). Since the parallelogram planes are vertical, so are sides $\boldsymbol{a}, \boldsymbol{b}, \boldsymbol{c}$ of the characteristic tetrahedron.

Since all sides are vertical, cases 5 to 9 in Table 1 can only occur if the mobile platform plane is also in a vertical orientation, since at least one of the sides $\boldsymbol{a}$, $\boldsymbol{b}$, $\boldsymbol{c}$ is coincident with the upper platform plane $\boldsymbol{d}$. Note that, for typical platform manipulators, these singularities are generally outside the limited range of motion. (Otherwise, this type of singularity can be detected by examining the angle between the three sides and the

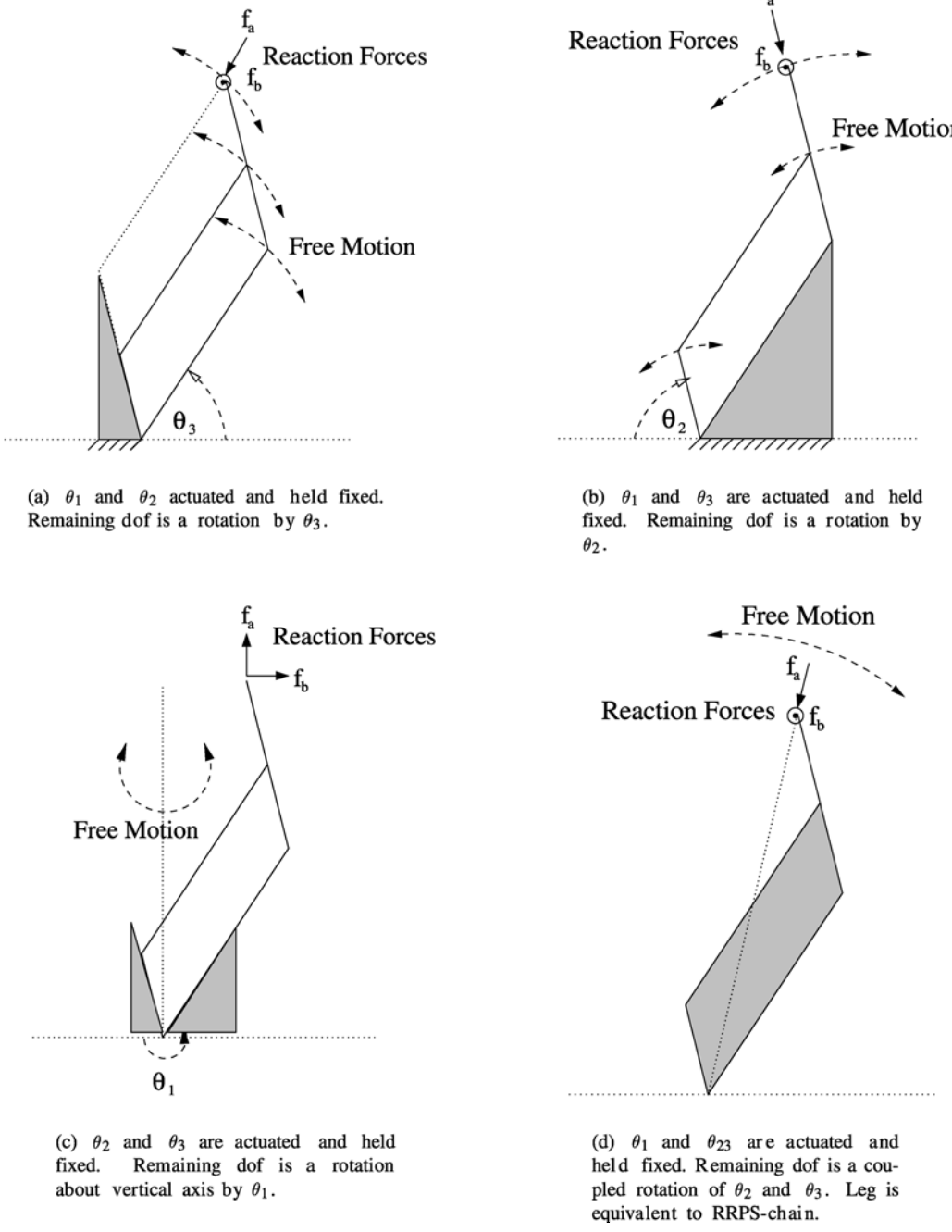

Fig. 8 Leg reaction forces and remaining degree of freedom for each of the four actuator placements. In (a), (b) and (d), f_B is normal to the parallelogram plane

mobile platform plane which can easily be calculated using the normal vectors.)

Furthermore, since the sides are vertical, cases 1 and 3 cannot occur since they induce additional degeneracies: the conditions of case 1 plus the fact that the sides are vertical imply the conditions of case 2; likewise, case 3 leads for this manipulator to the conditions of cases 4 or 8.

Consequently, cases 2 and 4 are the only cases to be considered to analyse the singularities of this manipulator. Both of these are actually possible for this manipulator. (For example, Fig. 9c demonstrates an

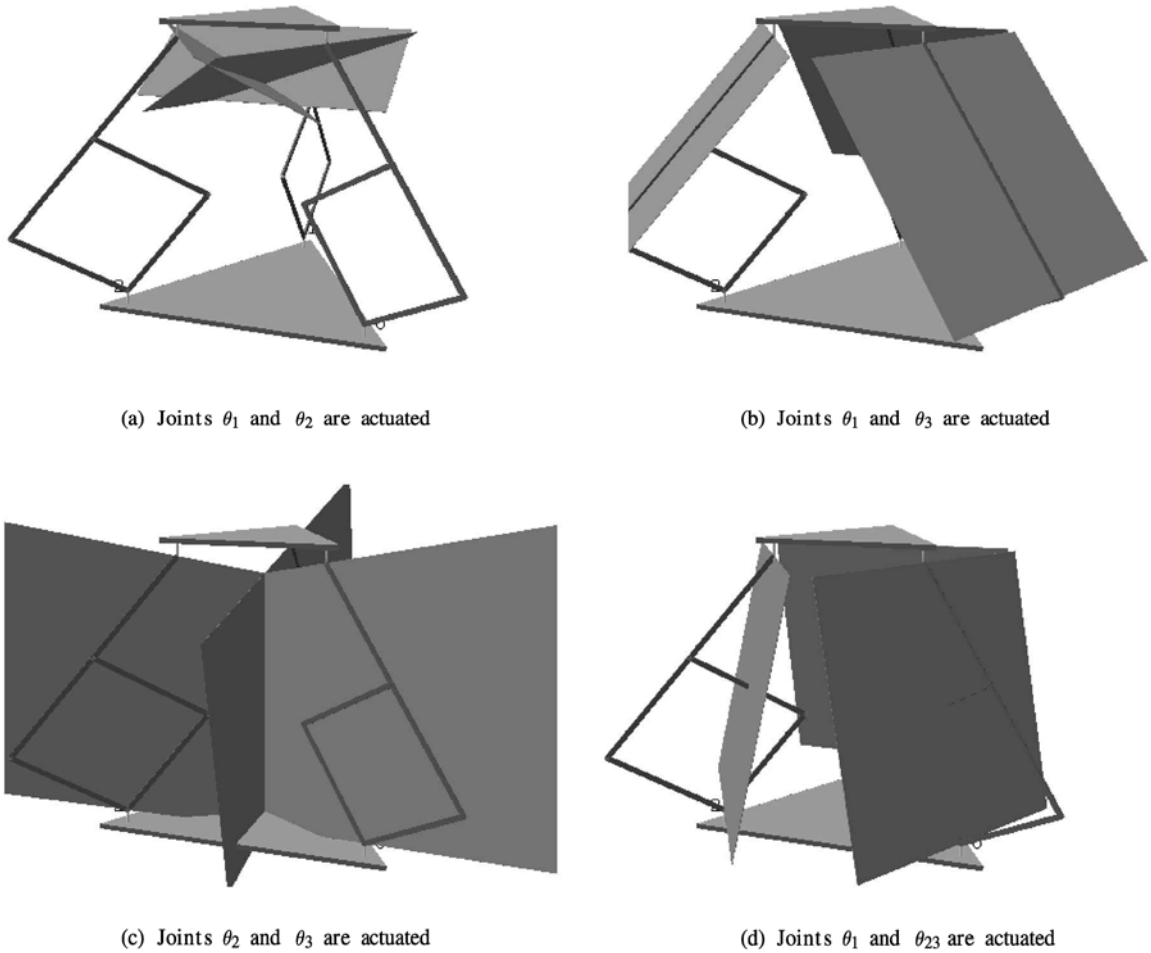

(a) Joints θ_1 and θ_2 are actuated

(b) Joints θ_1 and θ_3 are actuated

(c) Joints θ_2 and θ_3 are actuated

(d) Joints θ_1 and θ_{23} are actuated

Fig. 9 Planes corresponding to different actuator placement

example of case 2 where the three sides meet in a line.) The analysis of cases 2 and 4 is further simplified by letting $\boldsymbol{a}'$, $\boldsymbol{b}'$, $\boldsymbol{c}'$ denote the projections of $\boldsymbol{a}$, $\boldsymbol{b}$, $\boldsymbol{c}$ on to the x, y plane (see examples in Fig. 10). The manipulator is in a singular configuration if and only if the three lines, $\boldsymbol{a}'$, $\boldsymbol{b}'$, $\boldsymbol{c}'$, have a common intersection point, i.e. the area of the enclosed triangle is zero. This is a very intuitive and simple geometric criterion that can be applied for any configuration to determine whether it is singular.

It is interesting to examine the geometry when the lower and upper platforms are equilateral triangles. If the mobile upper platform is translated from the lower platform without rotation, it can be shown that sides $\boldsymbol{a}$, $\boldsymbol{b}$, $\boldsymbol{c}$ always intersect in a vertical line. This means it is in a singular configuration of case 2. It also provides an intuitive reason why the neutral position of this manipulator type is generally chosen such that the mobile platform is rotated by 60° about the vertical axis in order to be 'far away' from this set of singular configurations. In conclusion, for this type of manipulator, all singularity configurations can be identified from a simple geometric condition that is simple to compute and visualize.

6 CONCLUSIONS

This paper presents a new method for identifying wrench singularities. It is applicable to a common class of parallel manipulators that have three legs with up to two actuators each, and whose legs are connected to the mobile platform through spherical joints. The primary result shows that the manipulator is at a wrench singularity if and only if the characteristic tetrahedron is singular. The enumeration of singular tetrahedra leads to an enumeration of wrench singularities. In application to the sample manipulators, the tetrahedron is easily visualized and the different singularities are readily enumerated.

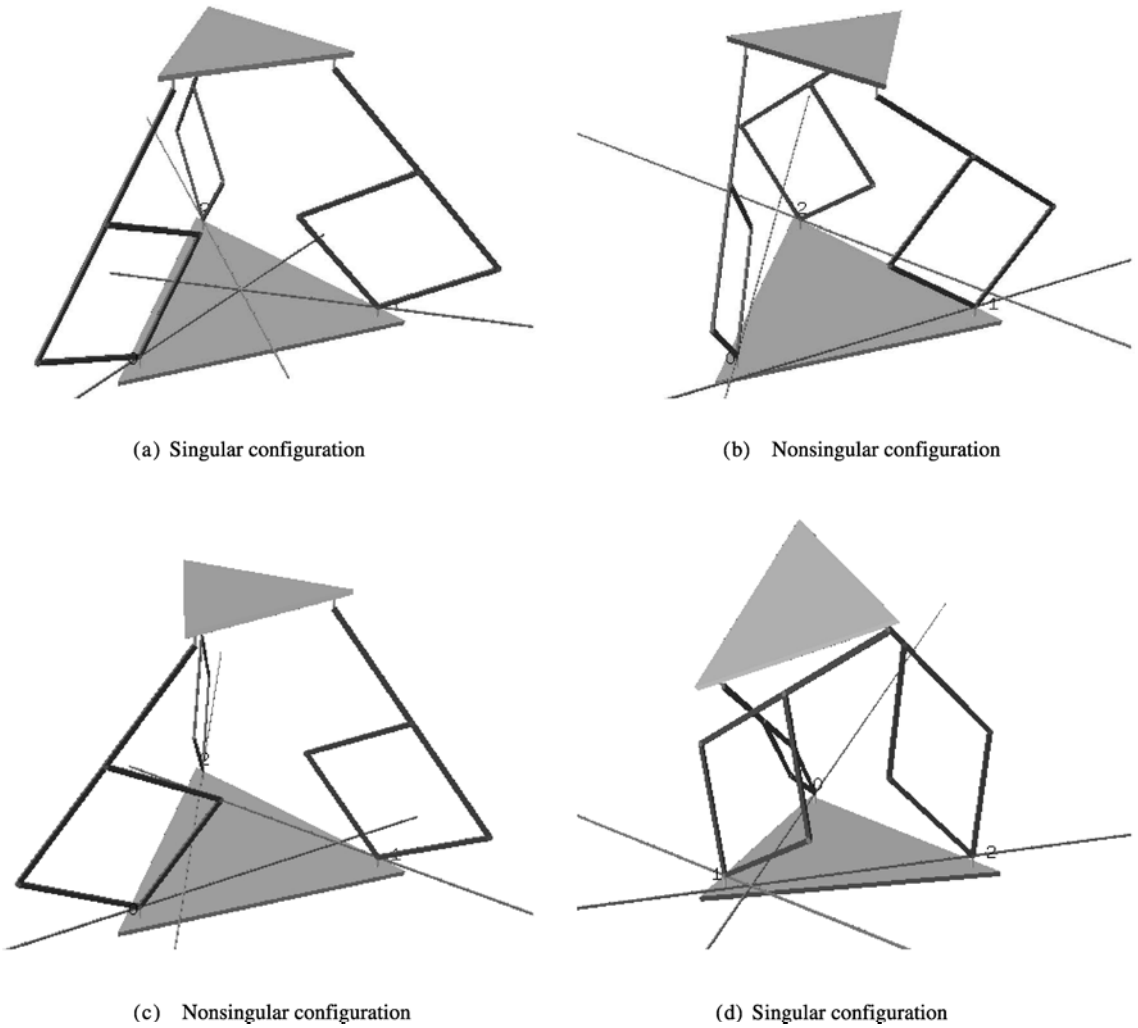

Fig. 10 Criterion for singularity: do the projections of three legs onto the base plane intersect at a single point?

ACKNOWLEDGEMENTS

The authors gratefully acknowledge the constructive comments of one of the reviewers, particularly for identifying cases not covered by the originally proposed enumeration method for singular configurations. Furthermore, this research was partly supported by NSF Award 9984279.

REFERENCES

1 **Klein, F.** *Elementary Mathematics from an Advanced Standpoint: Geometry*, 1939 (Dover Publications).
2 **Gosselin, C.** and **Angeles, J.** Singularity analysis of closed loop kinematic chains. *IEEE Trans. Robotics and Automn*, 1990, **6**(3), 281–290.
3 **Ball, R. S.** *Theory of Screws*, 1900 (Cambridge University Press).
4 **Hunt, K. H.** *Kinematic Geometry of Mechanisms*, 1978 (Oxford University Press).
5 **Phillips, J.** *Freedom in Machinery*, Vol. 1, *Introducing Screw Theory*, 1984 (Cambridge University Press).
6 **Phillips, J.** *Freedom in Machinery*, Vol. 2, *Screw Theory Exemplified*, 1990 (Cambridge University Press).
7 **Collins, C. L.** and **Long, G. L.** Singularity analysis of an in-parallel hand controller for force-reflected teleoperation. *IEEE Trans. Robotics and Automn*, 1995, **11**(5), 661–669.
8 **Hao, F.** and **McCarthy, J. M.** Conditions for line-based singularities in spatial platform manipulator. *J. Robotic Syst.*, 1998, **15**(1), 43–55.
9 **Merlet, J.-P.** Singular configurations of parallel manipulators and Grassmann geometry. *Int. J. Robotics Res.*, 1989, **8**(5), 45–56.
10 **Notash, L.** Uncertainty configurations of parallel manipulators. *Mech. Mach. Theory*, 1998, **33**(1–2), 123–138.
11 **Dandurand, A.** The rigidity of compound spatial grid. *Struct. Topology*, 1994, (10), 45–56.
12 **Zlatanov, D. S., Fenton, R. G.** and **Benhabib, B.** Analysis of the instantaneous kinematics and singular configurations

of hybrid-chain manipulators. In 1994 ASME Design Engineering Technical Conferences, Minneapolis, Minnesota, September 1994, DE-Vol. 72, pp. 467–476.

13 **Merlet, J.-P.** *Les robots parallèles. Collection Robotique*, 2nd edition, 1997 (Hermes, Paris).

14 **Lee, K. M.** and **Shah, D. K.** Kinematic analysis of a three-degrees-of-freedom in-parallel actuated manipulator. *IEEE J. Robotics and Automn*, 1988, **4**(3), 354–360.

15 **Lipkin, H.** Geometry and mappings of screws with applications to the hybrid control of robotic manipulators. PhD thesis, University of Florida, 1985.

16 **Lipkin, H.** and **Pohl, E.** Enumeration of singular configurations for robotic manipulators. *Trans. ASME, J. Mech. Des.*, September 1991, **113**, 272–279.

17 **Ebert-Uphoff, I.** and **Gosselin, C. M.** Kinematic study of a new type of spatial parallel platform mechanism. In 1998 ASME Design Engineering Technical Conferences, Atlanta, Georgia, September 1998, DETC/MECH-5962.

18 **Matone, R.** and **Roth, B.** In-parallel manipulators: a framework on how to model actuation schemes and a study of their effects on singular postures. In 1998 ASME Design Engineering Technical Conferences, Atlanta, Georgia, September 1998.